島根大学地球資源環境学研究報告　33, 1～8 ページ（2015 年 2 月）
Geoscience Rept. Shimane Univ., 33, p.1～8（2015）

Article

White micas from the Seba eclogitic basic schists in the Sambagawa metamorphic belt, central Shikoku, Japan

Naohito Kishira*, Akira Takasu* and Md. Fazle Kabir*

Abstract

The Seba eclogitic basic schists in the Besshi district of central Shikoku consist mainly of garnet, omphacite, sodic, sodic-calcic and calcic-amphiboles, epidote and phengite along with small amounts of chlorite, albite, quartz, rutile and titanite. Calcite and hematite occur occasionally. Phengites in the eclogites have three modes of occurrence (Ph 1-3). Phengites (Ph1) occurring in the matrix have a schistosity. Relatively thicker flakes of phengites (Ph2) occasionally grow oblique to the schistosity, and phengites (Ph3) replace porphyroblastic garnets along their rims and cracks. Phengites in the Sebadani area show extensive range of chemical compositions, suggesting a variety of equilibrium metamorphic *P-T* conditions. Phengites (Ph1) have higher in Si and a compositional zoning with increasing Si from core to rim, suggesting a prograde growth zoning. Therefore, phengites (Ph1) were probably crystallized during prograde to peak metamorphism in the eclogite facies. Some phengites in the matrix (Ph1) showing decreasing Si contents from core to rim are probably developed during the retrograde metamorphism of the eclogite. Phengites (Ph2) occurring with random orientation to the schistosity, and phengites (Ph3) replacing the porphyroblastic garnets suggest that eclogites in the Sebadani area also suffered another high-pressure metamorphism, that probably corresponds to the Sambagawa metamorphism of the epidote-amphibolite facies in the Besshi area.

Key words: Sambagawa (Sanbagawa) metamorphic belt, Seba eclogitic basic schists, eclogite, Besshi district, phengite

Introduction

The Sambagawa metamorphic belt is a high-pressure intermediate type metamorphic belt (Miyashiro, 1973), and it consists mainly of pelitic and basic schists with a small amount of siliceous and psammitic schists. The metamorphic grades range from the pumpellyite-actinolite facies through the blueschist / greenschist facies to the epidote-amphibolite facies (e.g. Banno, 1964; Higashino, 1990; Enami *et al.*, 1994).

The Sambagawa metamorphic belt developed in central Shikoku has been divided into four metamorphic zones based on the appearance of index minerals in pelitic schists, i.e. chlorite, garnet, albite-biotite and oligoclase-biotite zones, in ascending order of metamorphic grade (Enami, 1983; Higashino, 1990) (Fig. 1). The *P-T* conditions of each zone have been estimated as 300-360˚C / 5.5-6.5 kbar (chlorite zone), 425-470˚C / 7-8.5 kbar (garnet zone) and 470-590˚C / 8-9.5 kbar (albite-biotite zone) 585-635˚C / 9-11 kbar (oligoclase-biotite zones) (Enami, 1983; Enami *et al.*, 1994).

Several eclogite-bearing bodies occur throughout the albite-biotite and the oligoclase-biotite zones in the high-grade portions of the metamorphic sequence in the Besshi district (e.g. Yokoyama, 1980; Takasu, 1984; Kunugiza *et al.*, 1986; Takasu, 1989; Aoya, 2001; Kugimiya and Takasu, 2002; Ota *et al.*, 2004; Miyagi and Takasu, 2005; Kabir and Takasu, 2010a, b; Endo and Tsuboi, 2013) (Fig. 1). However, these eclogite-bearing bodies underwent extensive recrystallization under epidote-amphibolite facies conditions, they locally preserve evidence of the eclogite facies metamorphism (e.g. Takasu, 1989; Wallis and Aoya, 2000; Ota *et al.*, 2004; Kabir and Takasu, 2010a).

The Sebadani area located in the central part of the Besshi district, belongs to the albite-biotite zone. The Sebadani metagabbro mass and surrounding Seba basic schists (Seba eclogitic basic schists), pelitic and siliceous schists occur in the area (Takasu and Makino, 1980; Takasu, 1984). Eclogitic mineral assemblages are sporadically preserved in both the Sebadani metagabbro and the Seba basic schists (Seba eclogitic basic schists) (e.g. Takasu, 1984; Naohara and Aoya, 1997; Aoya, 2001).

Aoya (2001) reported a *P-T* path of the eclogites occurring in the Seba eclogitic basic schists. The eclogites first attained the peak pressure conditions, then decompressed with continuously increasing temperature until they reached the peak temperature conditions (610-640˚C and 12-24 kbar). The eclogites were then retrograded at epidote-amphibolite conditions, and were subsequently emplaced into surrounding non-eclogitic schists at the time of prograde epidote-amphibolite metamorphism (Aoya, 2001; Zaw Win Ko *et al.*, 2005).

The Onodani eclogites preserved within the Seba basic schists have a complex metamorphic history, undergoing three different metamorphic episodes (Kabir and Takasu, 2010a). The metamorphic conditions of the first and the second eclogite facies metamorphism are estimated to have been 530-590˚C and 19-21 kbar and 630-680˚C and 20-22 kbar, respectively. The second metamorphic event is similar to that of the Seba eclogitic basic schists (610-640˚C and 12-24 kbar)

*Department of Geoscience, Graduate School of Science and Engineering, Shimane University, 1060 Nishikawatsu, Matsue 690-8504, Japan

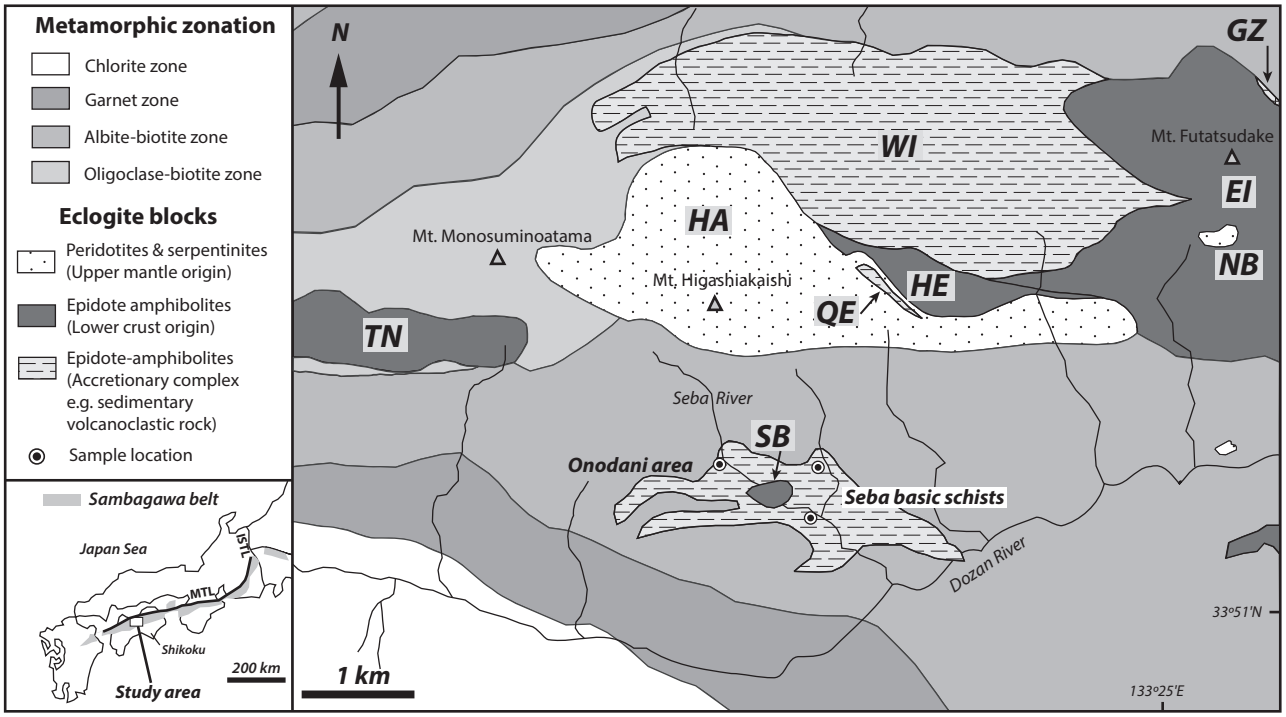

Fig. 1. Geological and metamorphic zonation map of the Sambagawa metamorphic belt in the Besshi district, central Shikoku, Japan (compiled from Takasu and Makino, 1980; Takasu, 1989; Higashino, 1990; Kugimiya and Takasu, 2002; Sakurai and Takasu, 2009; Kabir and Takasu, 2010a). SB, Seba metagabbro mass; TN, Tonaru metagabbro mass; WI, Western Iratsu mass; EI, Eastern Iratsu mass; HA, Higashi-akaishi peridotite mass; QE, Quartz eclogite mass; HE, Hornblende eclogite mass; NB, Nikubuchi peridotite mass; GZ, Gazo eclogite mass.

(Aoya, 2001). The pelitic schists intercalated within the Seba eclogitic basic schists also underwent eclogite facies metamorphism of 520-550˚C and c. 18 kbar (Zaw Win Ko *et al.*, 2005; Kouketsu *et al.*, 2010).

In this study we describe the modes of occurrence and chemistry of white micas in the eclogite from the Seba eclogitic basic schists. The mineral abbreviations used in the text, tables, and figures follow Whitney and Evans (2010).

Petrography of the Seba eclogitic basic schists

The eclogites found in the northeastern part of the Seba eclogitic basic schists have been petrographically described by Kishira *et al.* (2013). Phengites in the eclogite from the northeastern part occur in three modes of occurrence (Figs. 2a and 3). Firstly, phengites in the matrix (Ph1) as a schistosity-forming minerals are euhedral to subhedral grains up to 1 cm across, and they contain inclusions of epidote, omphacite, albite and calcite. Some of them are zoned with darker core and lighter rim in backscattered electron images (Fig. 3c-d). The other show opposite zoning. Secondly, phengites randomly oriented to the matrix schistosity (Ph2) are similar in size, although relatively thicker than schistosity-forming phengites, and they contain inclusions of titanite and calcite (Fig. 3a-b). The third type of phengites occurs as secondary mineral (Ph3) replacing porphyroblastic garnets along the rim and crack, and it contains titanite and calcite as inclusions (Figs. 2a and 3e-f).

Eclogites from the northwestern and central parts of the Seba eclogitic basic schists consist mainly of garnet, omphacite, sodic, sodic-calcic and calcic-amphiboles (glaucophane, winchite, barroisite, magnesiokatophorite magnesiotaramite, edenite, magnesiohornblende and pargasite), epidote, and phengite (Fig. 2b-c). The eclogites occurring in the northwestern and central parts are free from dolomite. Small amounts of chlorite, albite, quartz, rutile and titanite, calcite and hematite occur occasionally. A schistosity is defined by preferred orientation of omphacite, amphibole, epidote and phengite.

Garnets occur as euhedral to subhedral grains up to 1 mm in diameter (Fig. 2b-c). Some are zoned with pale pink core to colorless rim. The garnets contain inclusions of omphacite (X_{Jd} 0.24-0.29), hematite and quartz. Some garnets are partly replaced by chlorite. Omphacites occur as anhedral grains up to 1.2 mm across, and some are zoned from pale green core to colorless rim (X_{Jd} 0.24-0.37). The omphacites contain inclusions of amphibole (barroisite, magnesiokatophorite, magnesiohornblende), epidote, hematite, titanite and quartz, and they are partly replaced by amphibole (barroisite/edenite)+albite symplectite.

Schistosity-forming amphiboles occur as subhedral anhedral to grains up to 0.8 mm across, and some of them are zoned with resorbed winchite/barroisite/magnesiokatophorite core,

resorbed glaucophane mantle, barroisite/magnesiotaramite rim, and edenite/magnesiohornblende/pargasite outermost rim. Amphiboles in the matrix contain inclusions of omphacite (X_{Jd} 0.26-0.27), epidote, rutile, titanite, hematite and quartz. Epidote occurs as anhedral grains up to 0.8 mm across. They are zoned, from yellowish-green cores to colorless rims, and they contain hematite and quartz as inclusions.

Phengites (Ph1) occur only as a schistosity-forming mineral in the northwestern and central part of the Seba eclogitic basic schists, and they are of euhedral to subhedral grain up to 0.7 mm across (Fig. 2b-c).

Chemical compositions of the phengites

Chemical composition and compositional zoning of the phengites from the Seba eclogitic basic schists were investigated at Shimane University, using JEOL JXA 8800M and JXA 8530F electron microprobe analyzers. Analytical conditions used for quantitative analysis were 15 kV accelerating voltage, 20 nA specimen current, and 5 μm beam diameter. Correction procedure was carried out as described by Bence and Albee (1968). Representative chemical compositions of phengites are listed in Table 1, and shown in Fig. 4. Cr (<0.12 wt%) contents in the phengites are negligible.

Schistosity-forming phengites (Ph1) from the northeastern part of the Saba eclogitic basic schists have composition of Si (6.72-7.07 pfu), X_{Na} (Na/(Na+K)) (0.06-0.15), Fe+Mg (0.86-1.48 pfu) and Ti (0.03-0.05 pfu) (Fig. 4). Some phengites (Ph1) are zoned with increasing Si (6.77-6.95 pfu) and Fe+Mg (0.90-1.00 pfu) and decreasing X_{Na} (0.14-0.06), and the other (Ph1) show decreasing Si (7.06-6.72 pfu) and X_{Na} (0.11-0.07) and increasing Fe+Mg (0.99-1.48 pfu) from core to rim (Fig. 3c-d). Si in phengite (Ph1) in the central part of the Saba eclogitic basic schists are similar to that of the northeastern part (Si 6.87-7.02 pfu, X_{Na} 0.07-0.11, Fe+Mg 0.97-1.03 pfu and Ti 0.03-0.07 pfu), whereas phengites in the northwestern part show wide range and slightly higher of Si (Si 6.64-7.14 pfu, X_{Na} 0.05-0.11, Fe+Mg 0.97-1.15 pfu and Ti 0.02-0.05 pfu).

Randomly oriented phengites (Ph2) have a compositional range of Si (6.79-7.12 pfu), Fe+Mg (0.86-1.20 pfu), Ti (0.02-0.05 pfu) and X_{Na} (0.06-0.15). They are slightly higher in Si than phengites in the matrix (Ph1), although Ti and X_{Na} in both Ph1 and Ph2 are similar (Fig. 4). Phengites (Ph2) are zoned with increasing Si (6.87-7.12 pfu), Fe+Mg (0.97-1.09 pfu) and decreasing X_{Na} (0.10-0.06) from core to rim.

Phengites (Ph3) replacing garnets have wide range of composition and higher in Si (6.58-7.17 pfu) than any other phengites in the eclogites. X_{Na} (0.06-0.14), Fe+Mg (0.89-1.12 pfu) and Ti (0.01-0.05 pfu) are similar to those randomly oriented phengites (Fig. 4). Phengites (Ph3) are sometimes zoned, with increasing Si (6.83-7.11 pfu), Fe+Mg (0.92-1.01 pfu) and decreasing X_{Na} (0.12-0.06) from core to rim.

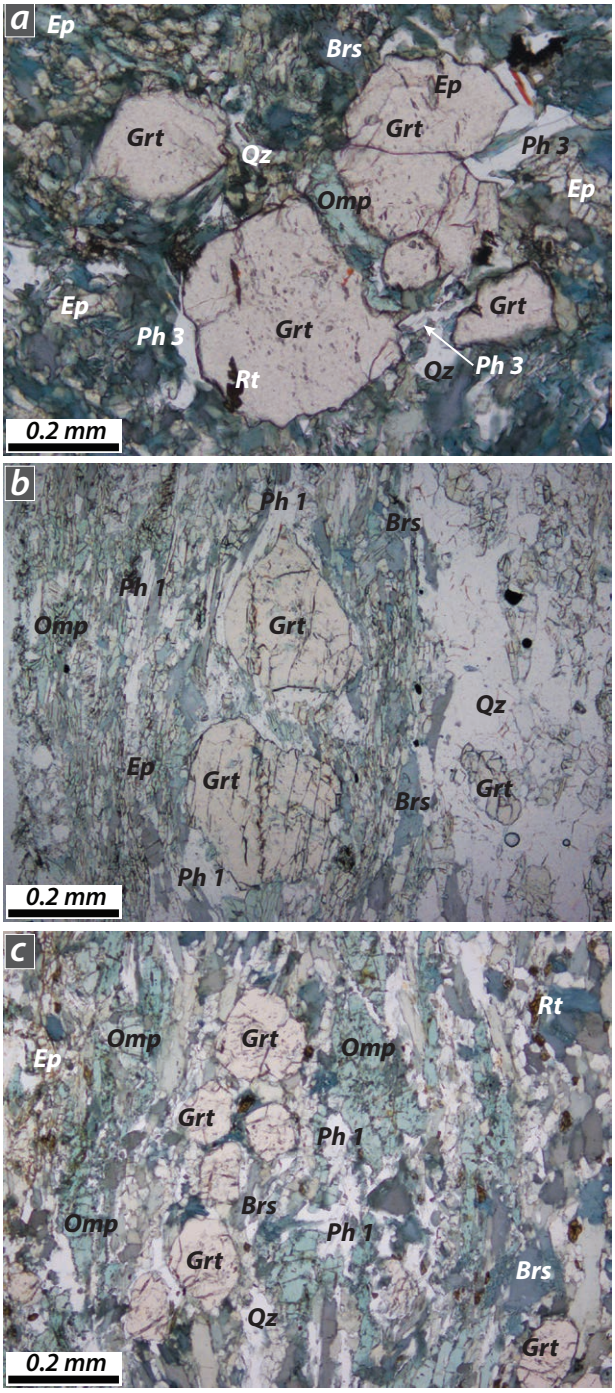

Fig. 2. Photomicrograph of eclogites from the Seba eclogitic basic schists. (a) Eclogite from the northeastern part (KSB 5) of eclogite showing eclogite facies mineral assemblages of porphyroblastic garnet and coexisting omphacite, phengite (Ph3), barroisitic amphibole and epidote. Garnets contain inclusions of epidote and rutile. (b) Eclogite from the northwestern part (KSB 42) showing schistosity-forming matrix minerals of porphyroblastic garnet, omphacite, barroisitic amphibole, phengite (Ph1), epidote and quartz. (c) Eclogite from the central part (KSB 48) showing porphyroblastic garnet and schistosity-forming omphacite, barroisitic amphibole, phengite (Ph1), epidote, rutile and quartz.

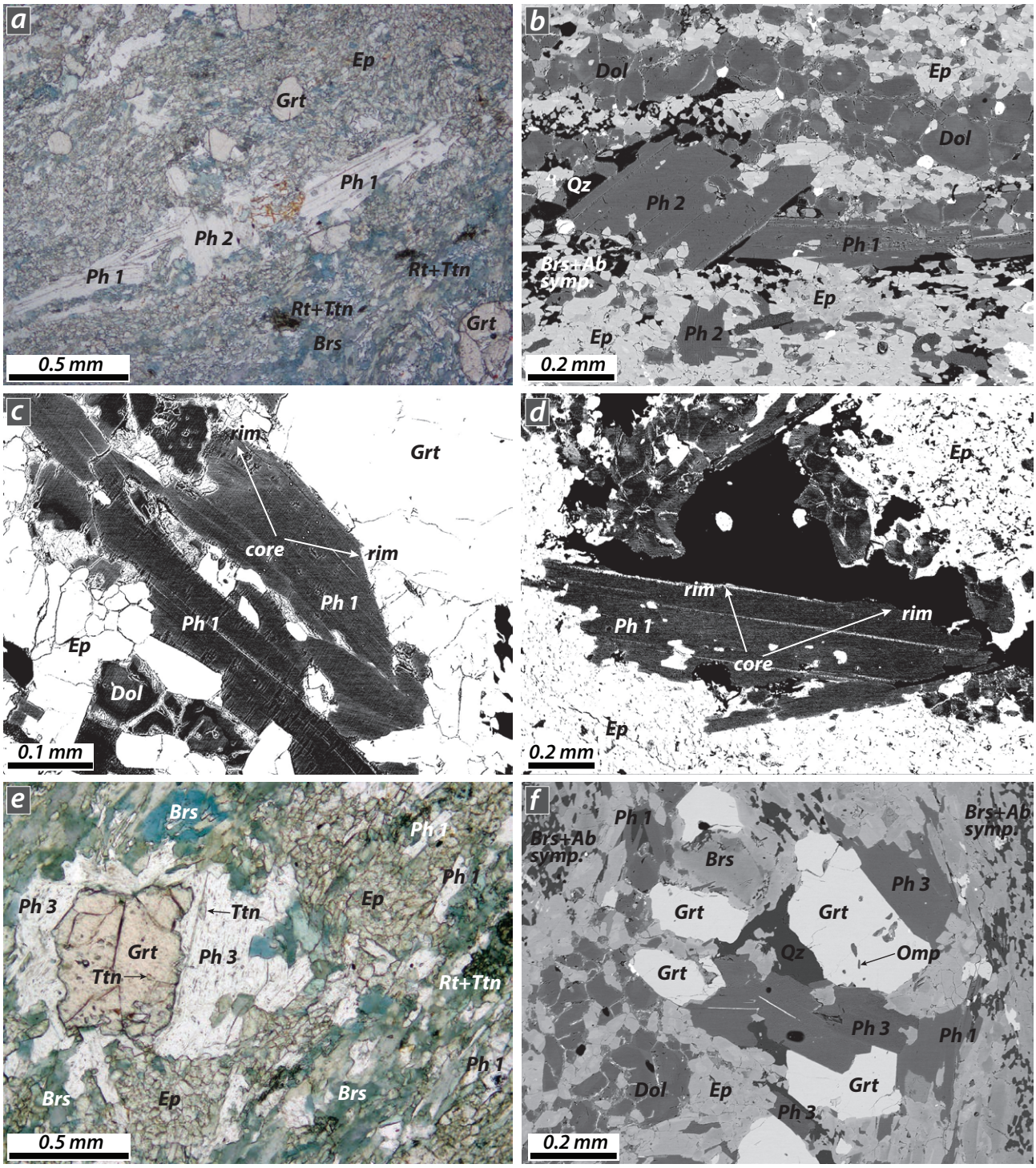

Fig. 3 Photomicrographs and backscattered electron images of the eclogites from the Seba eclogitic basic schists (a) Schistosity-forming matrix minerals of garnet, phengite (Ph1), barroisitic amphibole and epidote (KSB 5). Matrix rutiles are rimmed by titanite. Randomly oriented phengites (Ph2) are also shown. (b) Randomly oriented phengite (Ph2) and the other schistosity-forming matrix minerals of phengite (Ph1), epidote and dolomite (KSB 5). Several barroisite and albite symplectites are also shown. (c) Schistosity-forming phengite (Ph1) show compositional zoning with darker core to lighter rim (KSB 5). (d) Phengite (Ph1) show opposite zoning with lighter core to darker rim (KSB 42). (e) Schistosity-forming matrix minerals of garnet, phengite (Ph1), barroisitic amphibole and epidote (KSB 5). Porphyroblastic garnet is replaced by phengite (Ph3). Garnet contains inclusions of titanite and matrix rutiles are rimmed by titanite. (f) Showing matrix garnet, phengite (Ph1), barroisitic amphibole and epidote (KSB 5). Porphyroblastic garnet is replaced by phengite (Ph3). Garnet contains inclusions of omphacite and barroisite and albite symplectites are also shown.

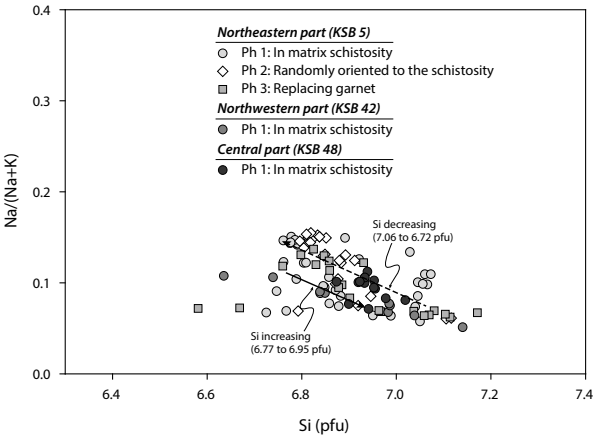

Fig. 4 Chemical compositions of phengites in the Seba eclogitic basic schists. Solidline arrow indicates Si contents in phengite (Ph1) increases and brokenline arrow indicates Si contents decreases from core to rim in the northeastern part of the Seba eclogitic basic schists.

Discussion and Conclusions

The modes of occurrence and chemical compositions of phengites in the eclogites from the Seba eclogitic basic schists (northeastern, northwestern and central parts) have been described. Phengites in the eclogites show three modes of occurrence and a wide range of chemical compositions.

Phengites (Ph1) have higher Si contents (6.64-7.14 pfu), and most of the phengites show compositional zoning with increasing Si contents from the core to the rim, suggesting a prograde growth zoning. Kabir and Takasu (2010c) reported matrix phengites represent prograde to peak metamorphism of the eclogite facies. The estimated peak metamorphic conditions of the eclogites from the Seba eclogitic basic schists are 12-24 kbar and 610-640˚C (Aoya, 2001; Kabir and Takasu, 2010c), and those of the second eclogite facies metamorphism of the Onodani eclogite are estimated to be 630-680˚C and 20-22 kbar (Kabir and Takasu, 2010a). Prograde zoned phengites (Ph1) probably suffered eclogite facies metamorphism similar to the prograde metamorphism shown by Kabir and Takasu (2010c). The other phengites (Ph1) showing decreasing Si contents from core to rim are probably developed during the retrograde metamorphism of the eclogite.

Randomly oriented phengites (Ph2) and phengites replacing garnets (Ph3) have wide range in Si (6.58-7.17 pfu) with increasing Si contents from core to rim, suggesting another high-pressure metamorphic event. The mode of occurrence of phengites probably corresponds to the third high-pressure metamorphic event reported by Kabir and Takasu (2010a, b), and suffered epidote-amphibolite facies metamorphism.

Acknowledgements

We thank members of the Geoscience and Metamorphic Geology Seminars of Shimane University for discussion and helpful suggestions and Hiroaki Komuro for critical reading and comments on the manuscript. Thanks are also due to Yasunori Kondo for his support during our fieldwork in the Besshi district. This study was partly supported by JSPS KAKENHI Grant (No. 24340123) to A.T.

Referrences

Aoya, M., 2001, *P-T-D* path of eclogite from the Sambagawa belt deduced from combination of petrological and microstructural analyses. *Journal of Petrology*, **42**, 1225-1248.

Bence, A. E. and Albee, A. L., 1968, Empirical correction factors for the electron microanalysis of silicates and oxides. *Journal of Geology*, **76**, 382-403.

Banno, S., 1964, Petrological studies of the Sanbagawa crystalline schists in the Bessi-Ino district, central Shikoku, Japan. *Journal of the Faculty of Science, Tokyo University, Section II*, **15**, 203-319.

Enami, M., 1983, Petrology of pelitic schists in the oligoclase-biotite zone of the Sanbagawa metamorphic terrain, Japan: phase equilibria in the highest grade zone of a high-pressure intermediate type of metamorphic belt. *Journal of Metamorphic Geology*, **1**, 141-161.

Enami, M., Wallis, S. R. and Banno, Y., 1994, Paragenesis of sodic pyroxene-bearing quartz schists: implications for the *P-T* history of the Sanbagawa belt. *Contributions to Mineralogy and Petrology*, **116**, 182-198.

Endo, S. and Tsuboi, M., 2013, Petrogenesis and implications of jadeite-bearing kyanite eclogite from the Sanbagawa belt (SW Japan). *Journal of Metamorphic Geology*, **31**, 647-661.

Higashino, T., 1990, The higher grade metamorphic zonation of the Sambagawa metamorphic belt in central Shikoku, Japan. *Journal of Metamorphic Geology*, **8**, 413-423.

Kabir, M. F. and Takasu, A., 2010a, Evidence for multiple burial-partial exhumation cycles from the Onodani eclogites in the Sambagawa metamorphic belt, central Shikoku, Japan. *Journal of Metamorphic Geology*, **28**, 873-893.

Kabir, M. F. and Takasu, A., 2010b, Glaucophanic amphibole in the Seba eclogitic basic schists, Sambagawa metamorphic belt, central Shikoku, Japan: implications for timing of juxtaposition of the eclogite body with the non-eclogite Sambagawa schists. *Earth Sciences*, **64**, 183-192.

Kabir, M. F. and Takasu, A., 2010c, Polyphase high-pressure metamorphism of eclogites and associated pelitic schists in the Sebadani and Onodani areas, Sambagawa metamorphic belt, central Shikoku, Japan. *Abstract for Annual Meeting, Japan Association of Mineralogical Sciences*, 205.

Kishira, N., Takasu, A. and Kabir, M. F., 2013, Modes of occurrence and chemical compositions of amphiboles in eclogite from the northeastern part of the Seba eclogitic basic schists in the Sambagawa metamorphic belt, central Shikoku, Japan. *Geoscience Reoprts of Shimane University,* **32**, 33-42.

Kouketsu, Y., Enami, M. and Mizukami, T., 2010, Omphacite-bearing metapelite from the Besshi region, Sambagawa metamorphic belt, Japan: Prograde eclogite facies metamorphism recorded in metasediment. *Journal of Mineralogical and Petrological Sciences*, **105**, 9-19.

Kugimiya, Y. and Takasu, A., 2002, Geology of the Western Iratsu mass within the tectonic melange zone in the Sambagawa metamorphic belt, Besshi district, central Shikoku, Japan. *Journal of the Geological Society of Japan*, **108**, 644-662.

Kunugiza, K., Takasu, A. and Banno, S., 1986, The origin and metamorphic history of the ultramafic and metagabbro bodies in the Sanbagawa Metamorphic Belt. *Geological Society of America Memoir*, **164**, 375-386.

Miyagi, Y. and Takasu, A., 2005, Prograde eclogites from the Tonaru epidote amphibolite mass in the Sambagawa Metamorphic Belt, central Shikoku, southwest Japan. *Island Arc*, **14**, 215-235.

Miyashiro, A., 1973, *Metamorphism and metamorphic belts*. George Allen and Unwin, London, England.

Naohara, R. and Aoya, M., 1997, Prograde eclogites from Sambagawa basic schists in the Sebadani area, central Shikoku, Japan. *Memoirs of the Faculty of Science and Engineering, Shimane University. Series A*, 63-73.

Ota, T., Terabayashi, M. and Katayama, I., 2004, Thermobaric structure and metamorphic evolution of the Iratsu eclogite body in the Sanbagawa belt, central Shikoku, Japan. *Lithos*, **73**, 95-126.

Sakurai, T. and Takasu, A., 2009, Geology and metamorphism of the Gazo mass (eclogite-bearing tectonic block) in the Sambagawa metamorphic belt, Besshi district, central Shikoku, Japan. *Journal of Geological Society of Japan*, **115**, 101-121.

Takasu, A., 1984, Prograde and retrograde eclogites in the Sambagawa metamorphic belt, Besshi district, Japan. *Journal of Petrology*, **25**, 619-643.

Takasu, A., 1989, *P-T* histories of peridotite and amphibolite tectonic blocks in the Sanbagawa metamorphic belt, Japan. In: *Evolution of Metamorphic Belts* (eds Daly, J. S., Cliff, R. A. & Yardley, B. W. D.), Geological Society, London, Special Publications, **43**, 533-538, Blackwell Scientific Publications, Oxford.

Takasu, A. and Makino, K., 1980, Stratigraphy and geologic structure of the Sanbagawa metamorphic belt in the Besshi district, Shikoku, Japan (Reexamination of the recumbent fold structures). *Earth Science*, **34**, 16-26 (in Japanese with English abstract).

Wallis, S. R. and Aoya, M., 2000, A re-evaluation of eclogite facies metamorphism in SW Japan: proposal for an eclogite nappe. *Journal of Metamorphic Geology*, **18**, 653-664.

Whitney, D. L. and Evans, B. W., 2010, Abbreviations for names of rock-forming minerals. *American Mineralogist*, **95**, 185-187.

Yokoyama, K., 1980, Nikubuchi peridotite body in the Sanbagawa metamorphic belt; thermal history of the 'Al-pyroxene-rich suite'peridotite body in high pressure metamorphic terrain. *Contributions to Mineralogy and Petrology*, **73**, 1-13.

Zaw Win Ko, Enami, M. and Aoya, M., 2005, Chloritoid and barroisite-bearing pelitic schists from the eclogite unit in the Besshi district, Sanbagawa metamorphic belt. *Lithos*, **81**, 79-100.

(Received: Oct. 10, 2014, Accepted: Jan. 16, 2015)

（要　旨）

岸良直人・高須　晃・Kabir Md. Fazle, 2014 四国中央部三波川変成帯瀬場エクロジャイト質塩基性片岩体中の白色雲母．島根大学地球資源環境学研究報告，33, 1-8.

四国中央部別子地域の三波川変成帯瀬場エクロジャイト質塩基性片岩中のエクロジャイトの主要構成鉱物は，ざくろ石，オンファス輝石，Na-, Na-Ca-, Ca- 角閃石，緑れん石，フェンジャイトである．微量成分鉱物として緑泥石，曹長石，石英，チタン石，ルチルが含まれる．また，まれに方解石と赤鉄鉱を伴う．エクロジャイト中のフェンジャイトには 3 つの産状がある (Ph 1-3). Ph1 は，片理を構成する．Ph2 は Ph1 よりも厚い幅をもち，片理に対して斜行して成長することがある．Ph3 は，斑状変晶のざくろ石のリムまたは割れ目を置換している．瀬場谷地域のエクロジャイト中のフェンジャイトは広い範囲の化学組成を示す．これはフェンジャイトが形成された平衡 P-T 条件の多様性を示唆する．Ph1 は高い Si 成分と，コアからリムへと Si の増加する組成累帯構造を示し，これは昇温期の成長累帯構造と考えられる．Ph1 は，おそらくエクロジャイト相変成作用の昇温期からピーク変成作用時の間に形成されたと考えられる．Ph1 にはコアからリムへ Si の減少を示すものがあり，これはピークのエクロジャイト相からの後退変成作用時に形成された可能性がある．片理に対してランダムな方向に形成されている Ph2 と，斑状変晶ざくろ石を置換する Ph3 は，エクロジャイト相変成作用の後に，緑れん石角閃岩相の三波川変成作用（狭義）を受けた間に形成されたと推定できる．

Table 1. Representative chemical compositions of phengites from the Seba eclogitic basic schists.

Sample	KSB 5																		
Analysis	68	69	70	71	72	73	74	75	76	77	78	83	84	85	86	87	88	89	90
Mode	Ph1	Ph1	Ph1	Ph1	Ph1	Ph1	Ph1	Ph1	Ph1	Ph1	Ph1	Ph1	Ph1	Ph1	Ph1	Ph1	Ph1	Ph1	Ph1
	Rim	←	←	←	Core	→	→	→	→	→	Rim	←	←	←	←	Core	→	→	→
SiO_2	51.67	50.93	51.19	50.66	50.36	53.00	52.64	51.57	51.03	51.34	51.18	51.74	51.96	51.47	50.81	50.96	50.78	51.09	50.32
TiO_2	0.31	0.34	0.41	0.38	0.41	0.27	0.34	0.43	0.36	0.48	0.43	0.38	0.33	0.48	0.43	0.40	0.38	0.40	0.39
Al_2O_3	27.38	27.38	27.56	26.21	28.39	25.78	26.56	28.38	28.75	28.69	28.59	27.39	27.64	28.56	28.60	28.04	27.86	27.33	28.21
FeO*	3.33	3.16	3.30	3.27	3.14	3.05	3.07	3.28	3.06	3.28	3.18	3.32	3.10	2.90	3.11	3.49	3.07	3.31	3.16
MnO	0.02	0.03	0.01	0.03	0.00	0.00	0.02	0.03	0.03	0.00	0.00	0.01	0.02	0.05	0.02	0.02	0.02	0.00	0.00
MgO	3.15	3.03	2.98	3.01	2.73	3.64	3.40	2.94	2.71	2.66	2.66	3.08	3.20	2.73	2.76	2.93	2.93	2.98	2.81
CaO	0.09	0.07	0.03	1.81	0.00	0.02	0.00	0.04	0.05	0.01	0.05	0.01	0.07	0.03	0.02	0.01	0.06	0.13	0.08
Na_2O	0.41	0.54	0.55	0.50	0.84	0.32	0.35	0.70	0.85	0.80	0.86	0.48	0.56	0.82	0.78	0.61	0.71	0.59	0.72
K_2O	7.76	7.84	7.87	7.88	7.47	7.88	7.75	7.62	7.28	7.37	7.57	7.85	7.69	7.46	7.10	7.93	7.71	7.57	7.76
Total	94.12	93.31	93.90	93.75	93.32	93.96	94.12	94.98	94.11	94.62	94.52	94.26	94.57	94.50	93.63	94.38	93.51	93.39	93.45
Cations on the basis of 22 oxygens																			
Si	6.88	6.85	6.85	6.84	6.76	7.05	6.99	6.81	6.78	6.79	6.79	6.88	6.88	6.81	6.78	6.79	6.81	6.86	6.76
Ti	0.03	0.03	0.04	0.04	0.04	0.03	0.03	0.04	0.04	0.05	0.04	0.04	0.03	0.05	0.04	0.04	0.04	0.04	0.04
Al	4.30	4.34	4.34	4.17	4.49	4.04	4.16	4.42	4.50	4.47	4.47	4.30	4.31	4.45	4.50	4.41	4.41	4.32	4.47
Fe*	0.37	0.36	0.37	0.37	0.35	0.34	0.34	0.36	0.34	0.36	0.35	0.37	0.34	0.32	0.35	0.39	0.34	0.37	0.36
Mn	0.00	0.00	0.00	0.00	0.00	0.00	0.00	0.00	0.00	0.00	0.00	0.00	0.00	0.01	0.00	0.00	0.00	0.00	0.00
Mg	0.63	0.61	0.59	0.61	0.55	0.72	0.67	0.58	0.54	0.52	0.53	0.61	0.63	0.54	0.55	0.58	0.59	0.60	0.56
Ca	0.01	0.01	0.00	0.26	0.00	0.00	0.00	0.01	0.01	0.00	0.01	0.00	0.01	0.00	0.00	0.00	0.01	0.02	0.01
Na2O	0.11	0.14	0.14	0.13	0.22	0.08	0.09	0.18	0.22	0.21	0.22	0.12	0.14	0.21	0.20	0.16	0.18	0.15	0.19
K	1.32	1.34	1.34	1.36	1.28	1.34	1.31	1.28	1.23	1.24	1.28	1.33	1.30	1.26	1.21	1.35	1.32	1.30	1.33
Total	13.65	13.69	13.68	13.78	13.70	13.61	13.60	13.67	13.66	13.65	13.69	13.66	13.65	13.65	13.63	13.72	13.70	13.66	13.72
X_{Na}	0.07	0.10	0.10	0.09	0.15	0.06	0.06	0.12	0.15	0.14	0.15	0.09	0.10	0.14	0.14	0.10	0.12	0.11	0.12

**Total Fe as FeO*

Sample	KSB 5																		
Analysis	91	92	8	9	10	11	12	13	14	15	16	17	18	19	20	44	45	46	47
Mode	Ph1	Ph1	Ph1	Ph1	Ph1	Ph1	Ph1	Ph1	Ph1	Ph1	Ph1	Ph1	Ph1	Ph1	Ph1	Ph2	Ph2	Ph2	Ph2
	→	Rim																	
SiO_2	50.76	52.24	52.09	54.42	49.32	53.66	54.00	54.20	54.18	54.12	54.17	52.00	50.62	53.73	52.95	50.58	53.11	50.90	51.54
TiO_2	0.37	0.46	0.38	0.36	0.33	0.33	0.35	0.35	0.36	0.36	0.29	0.27	0.35	0.28	0.27	0.37	0.32	0.48	0.45
Al_2O_3	28.45	27.84	27.52	26.56	25.52	26.31	26.54	26.41	26.43	26.63	25.94	27.54	26.67	26.22	27.55	26.91	27.43	28.04	28.31
FeO*	3.02	3.24	4.82	3.47	5.91	4.00	3.52	3.66	3.67	3.96	4.13	4.57	5.81	4.40	4.36	4.37	3.00	2.96	3.06
MnO	0.00	0.00	0.02	0.02	0.06	0.01	0.00	0.01	0.02	0.05	0.01	0.02	0.08	0.04	0.03	0.05	0.01	0.03	0.00
MgO	2.81	2.71	2.60	3.09	3.97	3.06	3.19	3.14	3.06	3.10	3.26	2.61	3.59	2.94	2.63	3.56	3.24	2.67	2.75
CaO	0.05	0.04	0.10	0.03	0.04	0.02	0.00	0.00	0.00	0.00	0.02	0.00	0.05	0.04	0.05	0.02	0.04	0.08	0.05
Na_2O	0.83	0.85	0.45	0.56	0.42	0.47	0.57	0.57	0.63	0.77	0.62	0.52	0.36	0.42	0.73	0.39	0.48	0.87	0.86
K_2O	7.48	7.35	8.20	7.84	8.92	7.60	7.70	7.91	7.74	7.58	7.62	7.76	7.45	8.01	7.67	7.92	7.87	7.49	7.53
Total	93.78	94.73	96.17	96.35	94.49	95.46	95.86	96.25	96.08	96.55	96.04	95.28	94.97	96.08	96.25	94.17	95.51	93.51	94.55
Cations on the basis of 22 oxygens																			
Si	6.78	6.89	6.86	7.07	6.73	7.05	7.05	7.06	7.06	7.03	7.08	6.88	6.78	7.04	6.92	6.80	6.95	6.82	6.82
Ti	0.04	0.05	0.04	0.04	0.03	0.03	0.03	0.03	0.03	0.03	0.03	0.03	0.04	0.03	0.03	0.04	0.03	0.05	0.05
Al	4.48	4.33	4.27	4.06	4.10	4.07	4.08	4.05	4.06	4.08	3.99	4.29	4.21	4.05	4.25	4.26	4.23	4.43	4.42
Fe*	0.34	0.36	0.53	0.38	0.67	0.44	0.38	0.40	0.40	0.43	0.45	0.51	0.65	0.48	0.48	0.49	0.33	0.33	0.34
Mn	0.00	0.00	0.00	0.00	0.01	0.00	0.00	0.00	0.00	0.00	0.00	0.00	0.01	0.00	0.00	0.01	0.00	0.00	0.00
Mg	0.56	0.53	0.51	0.60	0.81	0.60	0.62	0.61	0.59	0.60	0.64	0.51	0.72	0.57	0.51	0.71	0.63	0.53	0.54
Ca	0.01	0.01	0.01	0.00	0.01	0.00	0.00	0.00	0.00	0.00	0.00	0.00	0.01	0.01	0.01	0.00	0.01	0.01	0.01
Na2O	0.21	0.22	0.12	0.14	0.11	0.12	0.14	0.14	0.16	0.19	0.16	0.13	0.09	0.11	0.18	0.10	0.12	0.23	0.22
K	1.27	1.24	1.38	1.30	1.55	1.27	1.28	1.31	1.29	1.26	1.27	1.31	1.27	1.34	1.28	1.36	1.31	1.28	1.27
Total	13.69	13.62	13.72	13.59	14.02	13.58	13.59	13.61	13.60	13.62	13.61	13.67	13.77	13.63	13.66	13.77	13.62	13.67	13.67
X_{Na}	0.14	0.15	0.08	0.10	0.07	0.09	0.10	0.10	0.11	0.13	0.11	0.09	0.07	0.07	0.13	0.07	0.09	0.15	0.15

**Total Fe as FeO*

Sample	KSB 5																		
Analysis	48	49	50	51	52	54	55	56	57	58	59	60	61	62	63	1	2	3	4
Mode	Ph2	Ph2	Ph2	Ph2	Ph2	Ph2	Ph2	Ph2	Ph2	Ph2	Ph2	Ph2	Ph2	Ph2	Ph2	Ph2	Ph2	Ph2	Ph2
						Rim	←	←	←	Core	→	→	→	→	Rim				
SiO_2	51.58	51.53	52.10	51.94	52.42	52.58	51.75	51.93	51.47	51.37	51.65	51.87	51.82	51.72	52.01	54.03	51.25	51.58	52.36
TiO_2	0.38	0.37	0.42	0.47	0.47	0.33	0.52	0.32	0.35	0.38	0.41	0.44	0.43	0.45	0.34	0.23	0.26	0.26	0.37
Al_2O_3	27.44	28.05	28.44	28.43	28.41	27.42	28.44	27.77	27.88	28.42	28.23	28.74	28.77	28.75	27.84	25.79	27.04	27.41	27.30
FeO*	2.98	3.07	3.10	3.02	3.03	3.21	3.00	2.98	3.07	3.17	3.04	2.89	3.14	3.23	3.03	4.01	4.77	4.50	4.35
MnO	0.02	0.00	0.01	0.01	0.03	0.01	0.02	0.02	0.00	0.00	0.02	0.04	0.00	0.02	0.02	0.02	0.06	0.03	0.03
MgO	2.86	2.86	2.82	2.80	2.78	3.24	2.79	3.00	2.88	2.83	2.76	2.77	2.69	2.74	2.88	3.18	2.60	2.36	2.48
CaO	0.06	0.02	0.04	0.03	0.07	0.06	0.05	0.02	0.04	0.03	0.04	0.02	0.05	0.07	0.10	0.00	0.05	0.02	0.00
Na_2O	0.74	0.74	0.87	0.88	0.88	0.42	0.84	0.68	0.76	0.79	0.87	0.87	0.88	0.83	0.71	0.32	0.55	0.60	0.74
K_2O	7.48	7.50	7.50	7.41	7.63	7.92	7.53	7.47	7.62	7.52	7.46	7.25	7.35	7.41	7.56	7.57	7.58	7.88	7.91
Total	93.54	94.13	95.29	94.98	95.72	95.19	94.93	94.20	94.06	94.52	94.46	94.89	95.12	95.21	94.49	95.15	94.15	94.63	95.53
Cations on the basis of 22 oxygens																			
Si	6.90	6.85	6.84	6.84	6.85	6.92	6.82	6.89	6.85	6.81	6.84	6.82	6.81	6.80	6.88	7.11	6.87	6.88	6.91
Ti	0.04	0.04	0.04	0.05	0.05	0.03	0.05	0.03	0.03	0.04	0.04	0.04	0.04	0.04	0.03	0.02	0.03	0.03	0.04
Al	4.32	4.39	4.40	4.41	4.38	4.25	4.42	4.34	4.37	4.44	4.41	4.45	4.46	4.45	4.34	4.00	4.27	4.31	4.25
Fe*	0.33	0.34	0.34	0.33	0.33	0.35	0.33	0.33	0.34	0.35	0.34	0.32	0.35	0.36	0.34	0.44	0.53	0.50	0.48
Mn	0.00	0.00	0.00	0.00	0.00	0.00	0.00	0.00	0.00	0.00	0.00	0.00	0.00	0.00	0.00	0.00	0.01	0.00	0.00
Mg	0.57	0.57	0.55	0.55	0.54	0.64	0.55	0.59	0.57	0.56	0.54	0.54	0.53	0.54	0.57	0.62	0.52	0.47	0.49
Ca	0.01	0.00	0.01	0.00	0.01	0.01	0.01	0.00	0.01	0.00	0.01	0.00	0.01	0.01	0.01	0.00	0.01	0.00	0.00
Na2O	0.19	0.19	0.22	0.22	0.22	0.11	0.21	0.18	0.20	0.20	0.22	0.22	0.22	0.21	0.18	0.08	0.14	0.16	0.19
K	1.28	1.27	1.26	1.24	1.27	1.33	1.27	1.26	1.29	1.27	1.26	1.22	1.23	1.24	1.28	1.27	1.30	1.34	1.33
Total	13.64	13.65	13.66	13.65	13.66	13.64	13.66	13.63	13.67	13.67	13.66	13.63	13.64	13.66	13.64	13.55	13.68	13.69	13.69
X_{Na}	0.13	0.13	0.15	0.15	0.15	0.07	0.14	0.12	0.13	0.14	0.15	0.15	0.15	0.15	0.12	0.06	0.10	0.10	0.12

**Total Fe as FeO*

Table 1. (continued)

Sample	KSB 5																		
Analysis	5	22	24	25	26	27	28	29	34	35	36	37	38	39	40	41	42	23	24
Mode	Ph2	Ph3	Ph3	Ph3	Ph3	Ph3	Ph3	Ph3	Ph3	Ph3	Ph3	Ph3	Ph3	Ph3	Ph3	Ph3	Ph3	Ph3	Ph3
		Rim	←	Core	→	→	→	Rim	Rim	←	←	Core	→	→	→	→	Rim		
SiO_2	53.82	52.53	52.34	51.70	51.42	53.51	53.75	52.97	51.97	50.31	51.36	50.85	51.52	51.27	52.99	53.50	53.23	52.09	51.54
TiO_2	0.31	0.23	0.25	0.30	0.25	0.14	0.14	0.10	0.38	0.37	0.38	0.33	0.30	0.25	0.14	0.15	0.13	0.15	0.32
Al_2O_3	25.05	26.57	27.65	28.25	28.21	25.84	25.74	25.60	27.26	28.31	28.18	28.27	27.83	27.29	26.09	25.73	25.81	28.08	27.16
FeO*	3.83	4.37	3.23	3.41	3.47	3.28	3.06	3.08	4.20	3.93	3.55	3.54	3.56	3.61	3.23	2.82	3.14	4.10	3.78
MnO	0.01	0.02	0.00	0.03	0.04	0.00	0.02	0.03	0.04	0.04	0.00	0.01	0.00	0.00	0.05	0.01	0.09	0.01	0.02
MgO	3.36	2.86	2.71	2.59	2.68	3.40	3.42	3.35	2.67	2.39	2.53	2.59	2.75	2.72	3.38	3.47	3.46	2.59	2.92
CaO	0.01	0.05	0.00	0.01	0.03	0.03	0.05	0.16	0.02	0.14	0.02	0.00	0.03	0.08	0.02	0.03	0.17	0.02	0.00
Na_2O	0.36	0.39	0.69	0.74	0.68	0.39	0.34	0.38	0.46	0.66	0.79	0.74	0.69	0.55	0.39	0.36	0.37	0.66	0.56
K_2O	8.36	8.07	7.48	7.49	7.56	7.91	7.68	8.30	7.62	7.41	7.56	7.52	7.46	7.75	8.01	7.85	8.12	7.80	8.13
Total	95.11	95.09	94.34	94.52	94.33	94.50	94.20	93.97	94.61	93.54	94.37	93.84	94.14	93.52	94.31	93.92	94.51	95.48	94.42
Cations on the basis of 22 oxygens																			
Si	7.12	6.97	6.93	6.85	6.83	7.08	7.12	7.07	6.91	6.77	6.83	6.80	6.86	6.89	7.04	7.11	7.06	6.86	6.88
Ti	0.03	0.02	0.02	0.03	0.02	0.01	0.01	0.01	0.04	0.04	0.04	0.03	0.03	0.03	0.01	0.01	0.01	0.01	0.03
Al	3.91	4.15	4.32	4.41	4.42	4.03	4.02	4.03	4.27	4.49	4.42	4.46	4.37	4.32	4.09	4.03	4.03	4.36	4.27
Fe*	0.42	0.48	0.36	0.38	0.39	0.36	0.34	0.34	0.47	0.44	0.40	0.40	0.40	0.41	0.36	0.31	0.35	0.45	0.42
Mn	0.00	0.00	0.00	0.00	0.00	0.00	0.00	0.00	0.00	0.00	0.00	0.00	0.00	0.00	0.01	0.00	0.01	0.00	0.00
Mg	0.66	0.57	0.53	0.51	0.53	0.67	0.68	0.67	0.53	0.48	0.50	0.52	0.55	0.55	0.67	0.69	0.68	0.51	0.58
Ca	0.00	0.01	0.00	0.00	0.00	0.00	0.01	0.02	0.00	0.02	0.00	0.00	0.00	0.01	0.00	0.00	0.02	0.00	0.00
Na2O	0.09	0.10	0.18	0.19	0.17	0.10	0.09	0.10	0.12	0.17	0.20	0.19	0.18	0.14	0.10	0.09	0.09	0.17	0.14
K	1.41	1.37	1.26	1.27	1.28	1.34	1.30	1.41	1.29	1.27	1.28	1.28	1.27	1.33	1.36	1.33	1.37	1.31	1.38
Total	13.65	13.67	13.61	13.64	13.66	13.60	13.55	13.66	13.63	13.68	13.67	13.68	13.65	13.66	13.63	13.58	13.64	13.68	13.72
X_{Na}	0.06	0.07	0.12	0.13	0.12	0.07	0.06	0.06	0.08	0.12	0.14	0.13	0.12	0.10	0.07	0.07	0.06	0.11	0.09

**Total Fe as FeO*

Sample	KSB 5/KSB 42																		
Analysis	25	38	39	40	41	42	43	44	45	33	25	26	27	28	29	30	31	32	33
Mode	Ph3	Ph1	Ph1	Ph1	Ph1	Ph1	Ph1	Ph1	Ph1	Ph1	Ph1	Ph1	Ph1	Ph1	Ph1	Ph1	Ph1	Ph1	Ph1
		Rim	←	←	←	Core	→	→	Rim										
SiO_2	52.72	52.03	53.48	51.40	53.46	54.39	51.41	53.49	50.43	52.71	52.89	52.78	52.78	51.59	52.19	53.04	52.28	53.02	52.72
TiO_2	0.33	0.54	0.53	0.44	0.49	0.17	0.35	0.42	0.45	0.38	0.57	0.61	0.60	0.59	0.65	0.62	0.56	0.58	0.56
Al_2O_3	26.71	25.51	26.64	27.60	26.47	25.28	27.75	25.94	28.40	27.30	26.85	27.36	26.99	26.82	26.73	27.25	26.69	26.71	27.02
FeO*	3.49	3.95	3.77	3.54	3.82	3.44	3.49	3.49	3.60	4.06	3.98	3.64	3.78	3.77	3.70	3.87	4.00	4.16	3.70
MnO	0.05	0.02	0.02	0.02	0.03	0.03	0.00	0.00	0.04	0.01	0.02	0.00	0.01	0.03	0.04	0.02	0.01	0.03	0.02
MgO	3.34	3.54	3.37	3.13	3.64	3.97	3.22	3.71	3.03	2.95	2.98	2.93	2.95	2.99	2.95	2.98	2.92	2.91	3.02
CaO	0.00	0.22	0.03	0.04	0.05	0.01	0.02	0.13	0.02	0.00	0.05	0.05	0.08	0.06	0.06	0.05	0.05	0.05	0.04
Na_2O	0.39	0.36	0.40	0.47	0.41	0.26	0.49	0.34	0.58	0.48	0.52	0.56	0.55	0.62	0.56	0.60	0.60	0.44	0.50
K_2O	7.90	7.47	7.57	7.34	7.45	7.39	7.48	7.46	7.38	8.74	7.59	7.20	7.25	8.38	7.63	7.20	7.72	7.31	7.27
Total	94.93	93.62	95.81	93.95	95.81	94.94	94.21	94.98	93.93	96.61	95.44	95.13	94.99	94.84	94.50	95.64	94.83	95.20	94.83
Cations on the basis of 22 oxygens																			
Si	6.97	6.98	6.99	6.85	6.99	7.14	6.84	7.04	6.74	6.90	6.96	6.93	6.95	6.87	6.93	6.94	6.93	6.98	6.95
Ti	0.03	0.05	0.05	0.04	0.05	0.02	0.04	0.04	0.05	0.04	0.06	0.06	0.06	0.06	0.07	0.06	0.06	0.06	0.06
Al	4.16	4.04	4.11	4.34	4.08	3.91	4.35	4.02	4.47	4.21	4.16	4.24	4.19	4.21	4.19	4.20	4.17	4.14	4.20
Fe*	0.39	0.44	0.41	0.39	0.42	0.38	0.39	0.38	0.40	0.44	0.44	0.40	0.42	0.42	0.41	0.42	0.44	0.46	0.41
Mn	0.01	0.00	0.00	0.00	0.00	0.00	0.00	0.00	0.00	0.00	0.00	0.00	0.00	0.00	0.00	0.00	0.00	0.00	0.00
Mg	0.66	0.71	0.66	0.62	0.71	0.78	0.64	0.73	0.60	0.58	0.58	0.57	0.58	0.59	0.58	0.58	0.58	0.57	0.59
Ca	0.00	0.03	0.00	0.01	0.01	0.00	0.00	0.02	0.00	0.00	0.01	0.01	0.01	0.01	0.01	0.01	0.01	0.01	0.01
Na2O	0.10	0.09	0.10	0.12	0.10	0.07	0.13	0.09	0.15	0.12	0.13	0.14	0.14	0.16	0.14	0.15	0.15	0.11	0.13
K	1.33	1.28	1.26	1.25	1.24	1.24	1.27	1.25	1.26	1.46	1.27	1.21	1.22	1.42	1.29	1.20	1.31	1.23	1.22
Total	13.64	13.63	13.59	13.62	13.60	13.54	13.65	13.58	13.68	13.75	13.61	13.56	13.57	13.75	13.63	13.57	13.65	13.56	13.57
X_{Na}	0.07	0.07	0.08	0.09	0.08	0.05	0.09	0.06	0.11	0.08	0.09	0.11	0.10	0.10	0.10	0.11	0.11	0.08	0.09

**Total Fe as FeO*